ITM Web of Conferences **67**, 01033 (2024) https://doi.org/10.1051/itmconf/20246701033
*ICMSA 2024*

# Most suitable threshold method for extremes in financial data with different volatility levels

*Retselisitsoe* Mosala[1], *Kgoane Agreement* Rachuene[1], and *Sandile Charles* Shongwe[2*]

[1]Department of Actuarial Science, Faculty of Commerce, University of Cape Town, South Africa.
[2]Department of Mathematical Statistics and Actuarial Science, Faculty of Natural and Agricultural Sciences, University of the Free State, South Africa.

**Abstract.** Estimating the threshold for extreme values is essential for anticipating and managing rare and impactful events. This paper discusses four different graphical methods of estimating thresholds using three different stock price datasets. The datasets have different levels of volatility (classified as low, medium, and high). For each of the datasets, thresholds are estimated, and a generalised Pareto distribution is then fitted to the exceedances above each threshold. Subsequently, the mean squared error is calculated for each fitted model, which is then used together with the number of exceedances for each respective threshold as criteria to analyse and make inferences on the most suitable threshold approach when using a dataset that has a specified degree of volatility. It was observed that when dealing with a dataset with low volatility, Pickand plot should be considered for threshold setting. When volatility is very moderate or high, using Hill plot to determine thresholds for extreme values is recommended. The motivation for this paper lies in the need to explore and identify the most effective threshold estimation methods when dealing with different levels of stock price volatility.

## 1 Introduction

Extreme value theory (EVT) is defined as the field of study that deals with the distribution of very high quantiles of data [1]. It was developed to estimate the probability of the occurrence of extremes and rare events as it allows for extrapolation of the behaviour of the probability distribution tails using large observations. With the rarity of such events, the normal distribution overlooks it and tends to focus on the bulk data in the middle (average), whilst EVT appears to solve such problems by highlighting the extreme part of the data (right tail). It is a blend of an enormous variety of applications involving different industries such as: (see Chapter 1 of [2]): floods, the size of freak waves, tornado outbreaks, maximum sizes of ecological populations, side effects of drugs, equity risks, day-to-day market risk, epidemics; and more importantly for the focus of this research work, the magnitude of changes in share prices.

In the context of actuarial science / insurance, extreme events may be considered as large claims because of catastrophic events like natural catastrophes such as the floods, man-made

*Corresponding author: shongwesc@ufs.ac.za

catastrophes such as aeroplane crashes and financial events such as stock market crashes. Some insurers with reinsurance arrangements may consider extreme events as extremely large claims that exceed the maximum threshold covered by the reinsurer. It is quite important to consider a series of insurance claims as any of the loss distributions [3], this is because insurance is centred around the principle of independence (low correlation between claims) and the law of large numbers [4].

In Chapter 8 of [1], it is stated that there are two models that are frequently used in operational risk modelling, block maxima model and the peak over threshold (POT), see also [5-6]. The two methods use the Generalised Extreme Value (GEV) and Generalised Pareto Distribution (GPD), respectively. These give a more accurate description of the tail distribution, [7]. The GEV distribution has three forms: the Gumbel, Fretchet and Weibull, whereas the POT approach to extreme value analysis is based on a Poisson process hence it uses the GPD [8]. These methodologies are more effective in capturing and representing extreme occurrences. Other studies by [9-16] have discussed the application of different EVT probability distributions in different contexts. For instance, [9-12] separately applied the GPD, GEV as well as GPD with extreme value Gumbel copula to assess the extreme tail behaviour of the returns calculated from the South African Financial Index (J580), South African Industrial Index (J520) and Bitcoin prices. Note that while [12] studied Bitcoin return for both gains and losses over the period 2008 to 2023; however, [13] studied only the Bitcoin returns for losses for the period 2017 to 2019 – both applied the GPD only. Next, [14] applied the GEVD and GPD to model the returns of the Bank of Kigali's (BK) stock, while [15] investigated the use of different threshold methods in quantifying market risk using S&P500 data as well as applying backtesting technique. Very helpful R software packages for EVT analysis are described in [16].

Identifying which data points from the entire dataset could be classified as extreme events is a critical aspect, and the choice of a threshold is pivotal in this process. If the estimated threshold, denoted as u, is set too high, we would observe only a limited number of values surpassing this threshold. Consequently, this would result in a substantial variance in the estimator for the threshold. If the threshold is too small, we would have a high number of exceedances and therefore invalidate the analysis of extreme events [7]. Thus, the most suitable threshold could be chosen by quantifying a trade-off between biasness and variance. The most suitable threshold should be neither too high nor too low. Numerous methods have been proposed for threshold estimation. The motivation behind undertaking this study arises from the recognition of a critical research gap of no scant scholarly literature that systematically evaluates the comparative performance of these methods, particularly in the context of datasets characterised by substantial variations in volatility.

The rest of the paper is structured as follows: Section 2, discusses the theory behind threshold exceedance, various methods that are used to estimate threshold value and the bias-variance trade-off. Next, Section 3, provides methodology and data for this paper. Section 4 provides the results of our study. Finally, Section 5 provides concluding remarks.

## 2 Methodology

### 2.1 Peak-over-threshold (PoT)

Suppose that $K$ is a random variable that is defined as follows: $K = X - u|X > u$. Then the cumulative distribution function, $G(k)$ is defined as [8]:

$$G(k) = P(K \leq k) = P(X - u \leq k|X > u) = P(X \leq k + u|X > u) = \frac{P(u < X < k + u)}{P(X > u)}$$

or equivalently, this can be written as,

$$G(k) = \frac{F(k+u) - F(u)}{1 - F(u)} \tag{1}$$

Differentiation of (1) yields

$$\frac{d}{dk}G(k) = \frac{f(k+u)}{1 - F(u)} \tag{2}$$

The GPD, which is used in conjunction to the POT is defined as:

$$G(k) = \begin{cases} 1 - \left(1 + \frac{k}{\gamma\beta}\right)^{-\gamma} & if\ \gamma \neq 0 \\ 1 - \exp\left(-\frac{k}{\beta}\right) & if\ \gamma = 0 \end{cases} \tag{3}$$

where $\beta \geq 0$ is a scale parameter and $\gamma$ is the shape parameter. The differentiated version of the GPD would be:

$$g(k) = \begin{cases} \frac{1}{\beta}\left(1 + \frac{x}{\gamma\beta}\right)^{-(\gamma+1)} & if\ \gamma \neq 0 \\ \frac{1}{\beta}\exp\left(-\frac{x}{\beta}\right) & if\ \gamma = 0 \end{cases} \tag{4}$$

The GPD in the case of $\gamma = 0$ is the exponential with $\lambda = 1/\beta$. These parameters can be estimated by the maximum likelihood method.

There are various methods to estimate the threshold, these can broadly be classified as graphical diagnostics, rules of thumb, probabilistic results, computational approaches, and a mixture of the listed models [17]. Selection of a threshold $u$ should not be seen as an easy task, as literature has shown that it influences parameter estimation [18]. Graphical approaches for threshold selection refer to the case where the entire population data is plotted on a graph, necessary diagnostics are performed, judgement is made, and conclusions are drawn with regards to the value that our threshold is going to take for modelling the extreme data [17]. Various methodologies have been proposed for estimating threshold values in the context of extreme event analysis.

For the purposes of this study, we will use the four threshold estimators (i.e., Hill plot, sample mean excess plot, dispersion index plot and Pickand plot) because studies have shown that they produce better results, are clear and consistent, and frequently offer a good solution to problematic situations, particularly when the volatility of the distribution varies over time.

## 2.2 Description of four graphical threshold estimation methods

### *2.2.1 Hill plot*

Hill plot is graphical representation designed for positive data and illustrates the Hill estimator for various order statistics values [2]. Additionally, it exhibits confidence intervals under the assumption of Pareto tails. The Hill estimator of the tail index $1/\gamma$ using $k+1$ order statistics, with a plot of the Hill estimator defined by $H_{k,n}$ as follows:

$$H_{k,n} = \frac{1}{\gamma} = \frac{1}{k}\sum_{j=1}^{k}(\ln X_{j,n} - X_{k,n}) \tag{5}$$

for $k > 2$. The threshold choice can be challenging, and parameter estimates can be sensitive to the threshold choice, there has been various improvement to the Hill plot. The threshold should be chosen such that the plot exhibits a predominantly linear trend above this specific threshold.

### *2.2.2 Sample mean excess plot*

Sample mean excess plot are also referred to as the mean residual life plot, this graphical representation serves as a diagnostic tool for the GPD and aids in threshold selection [2]. When the plot exhibits a flat pattern, it suggests a potential fit with exponential data, whereas a curved shape suggests that Weibull or gamma distributions may be more suitable for modelling. It's important to note that this plot often displays fewer observations on the right-hand side, resulting in increased variability in the confidence intervals depicted within the plot. The sample mean excess function is defined as follows:

$$e(u) = E(X - u|X > u) = \frac{\beta + \frac{1}{\gamma}u}{1 - \frac{1}{\gamma}} \tag{6}$$

where $\beta + \frac{1}{\gamma}u > 0$ and $\frac{1}{\gamma} < 1$. This function would establish the behaviour of the distribution tails. We use a graph to choose the optimal threshold, $u$, such that $u > 0$ while ensuring that the mean excess function is linear for $x$ and $u$. The turning point is a good choice for the optimal threshold and the QQ-plots would enable us to evaluate the goodness of fit, wherein, a concave series of data points would show a heavy-tailed distribution, but a convex would indicate a thin tail.

### *2.2.3 Dispersion index plot*

When dealing with data that has a time series, [19] proposed a threshold selection method that assumed that data above the threshold had Poisson distribution and the data was independent. This is especially true for extreme types of data. That is, let $X \sim Pois(\lambda)$, with $P[X = x] = \frac{e^{-\lambda} \times \lambda^x}{x!}$, where $E[X] = Var[X]$ and $x \in \mathbb{N}$. Using the dispersion index (DI)

$$DI = \frac{\sigma^2}{\mu} \tag{7}$$

where $\sigma^2$ is the Poisson distribution intensity and $\mu$ is the average of number of events in a specific period (usually a year). The goal is to have a ratio approximately equal to $1$, which suggests that $\sigma^2$ should be approximately equal to $\lambda$. If that is the case, then the population sample can then be modelled using the corresponding threshold by the Poisson distribution.

### *2.2.4 Pickand plot*

Pickand plot portrays Pickand estimator for different x-values ($k$, the order statistics). The approach considers negative data while disregarding any missing data [2]. It is explicitly established for the order denoted as '$k$' ranging from 1 up to the floor division of '$n$' by 4. Any fractional values arising from computations are truncated. Furthermore, the graphical representation also encompasses confidence intervals, predicated upon the assumption of a Pareto tail distribution.

## **2.3 Bias-Variance trade-off**

The bias-variance trade-off (often referred to as mean squared error, MSE) discussed in [20], is critical in understanding prediction errors (bias and variance) whenever model prediction is discussed. The capacity of a model to minimize bias and variance must be balanced. Gaining an in-depth knowledge of these flaws can assist us not only in developing correct models but also in avoiding the errors of overfitting and underfitting. In this paper, this trade-off will be used as a criterion in deciding which threshold estimation approach seems to give a more optimal threshold for each dataset. The MSE decomposes into a bias and variance component:

$$MSE = Bias^2 + Variance. \tag{8}$$

In simple terms, we will estimate a threshold then get exceedances that will then be modelled using GPD, and then afterward we calculate the MSE of the model. We will repeat this process for each threshold estimation method, the main goal is to find the model with small MSE while also taking into account the number of exceedances used to fit GPD. The threshold estimation method with the lowest MSE and sufficient exceedances would then be considered optimal for that specific dataset.

## 3 Mixture models on trimmed data

### 3.1 Descriptives

We originally studied and analysed many investment classes ranging from government bonds to equities of different entities that are listed on the Johannesburg Stock Exchange (JSE). Consequently, we decided to focus on the following three datasets that are listed on the JSE extracted from www.bloomberg.com:

- Transaction Capital Risk Services (TCRS) – The company focuses on investing and operating high-potential businesses in the market with historically low levels of client service and trust.
- Discovery Limited (Discovery) – The company offers life and health insurance, medical aid administration, science-based wellness programs, credit cards and investment products.
- South African Government Bond (SAGB) – They are issued by South African government to raise capital to finance its financial deficit.

Let $\{p_t\}$ be the time series of the daily price of financial assets under observation from January 2018 to June 2023. Figure 1 displays different stock prices $(p_t)$ for the selected entities and it shows different levels of noise.

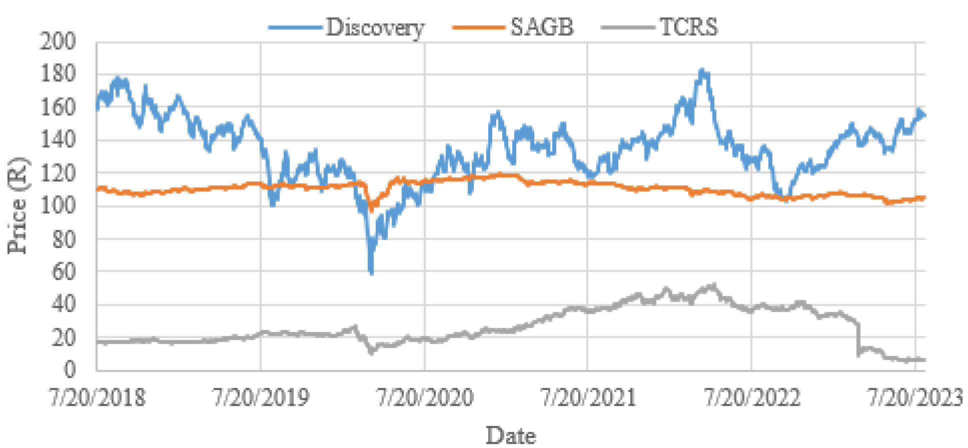


**Fig.1.** A time series of the stock prices of the TCRS, SAGB and Discovery.

When analyzing financial data, it is recommended to use returns ($r_t$) defined as [21]:

$$r_t = \log(p_t) - \log(p_{t-1}) \quad (9)$$

Next, Figure 2 provides the time series plot of the returns for each of the stock prices and their corresponding box plot summary in Figure 3. Thereafter the descriptives of $r_t$ are given in Table 1. In the last row of Table 1, all the $p$-values for the $r_t$ of the financial assets under consideration are all less than 0.05 which means under 95% confidence interval, we have enough evidence to reject the null hypothesis (time series contains a unit root and is non-stationary), thus, the time series are stationary. Stationary of the dataset does not mean it is identically and independently distributed (IID), it only implies that the data is identically distributed, and it says nothing about the independence.

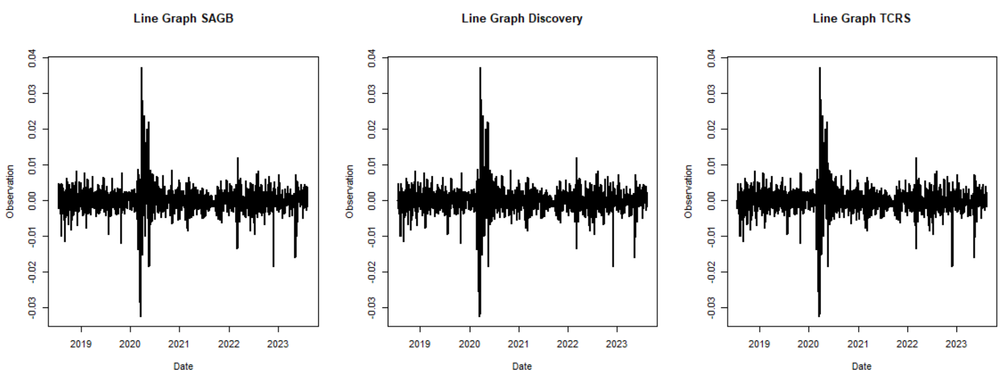


**Fig.2.** Stationary time series of all datasets.

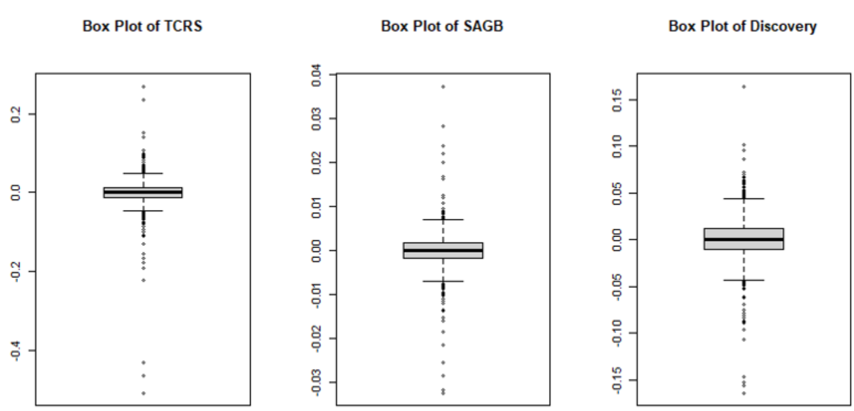


**Fig.3.** Box plots of all datasets.

**Table 1.** Statistical properties of the datasets.

| Statistic | TCRS | SAGB | Discovery |
|---|---|---|---|
| Sample size | 1265 | 1265 | 1265 |
| Minimum | −0,5085 | −0,0325 | −0,1637 |
| Maximum | 0,2699 | 0,0374 | 0,1640 |
| Percentile (90%) | 0,02655 | 0,0036 | 0,0237 |
| No. of obs in the upper 90% percentile | 127 | 127 | 127 |
| Mean | −0.0008 | −0.00004266 | −0.0000189 |
| Variance | 0,0013 | 0.000017 | 0,0005 |
| Standard deviation | 0,0366 | 0,0041 | 0,0234 |

| | | | |
|---|---|---|---|
| Kurtosis | 69.9926 | 19.6848 | 9.1021 |
| ADF test ($p$-value) | 0.01 | 0.01 | 0.01 |

As can be seen in Table 1, all the datasets under consideration have a sample size of 1265 and a notably 127 observations each in the upper tail region surpassing the 90th percentile. The evident presence of high positive kurtosis values within these datasets serves as a distinct indicator of their possessing heavy-tailed distributions, thereby implying an increased propensity for the occurrence of extreme events. The fundamental role of the standard deviation arises due to its integral function in classifying the degree of data volatility. To ensure that we account for different levels of volatility, we have undertaken an examination of various levels of volatility, thereby segregating these levels based on the standard deviation as the effective system of measurement. This approach allows for a coherent explanation of volatility across the different datasets: low, moderate and high levels defined by $[0, 0.015)$, $[0.015, 0.03)$ and $\geq 0.03$, respectively. From the standard deviation in Table 1, it becomes evident that the returns of the SAGB exhibits a noticeably low level of volatility, compared with the Discovery which exhibits a moderate level of volatility, while the TCRS demonstrates a relatively high level of volatility.

### 3.2 Threshold selection methods

An in-depth examination of four threshold selection methods is presented: Sample mean excess plot, Hill plot, dispersion index plot and Pickand plot.

#### *3.2.1 Sample mean excess plot*

The sample mean excess plot gives a threshold where the graph has a positive linear slope. This subsection will show a series of sample mean excess plots for the three different data sets followed by an interpretation of the optimal threshold. In Figure 4, the $y$-axis provides the sample mean excesses, which represent the average of observations exceeding a given threshold. Meanwhile, the $x$-axis describes the threshold values, which are the variables of primary interest. The mean excess plot of TCRS exhibits an initial declining trend, signifying a prevalence of numerous extreme events when the threshold resides in that specific range. Subsequently, after the appearance of the red line, the plot demonstrates an ascending trend, suggesting that extreme events become less frequent in this domain. Consequently, the optimal threshold point corresponds to a turning point, or a region characterized by graph stability, which, in this case, lies in proximity to the location of the red line.

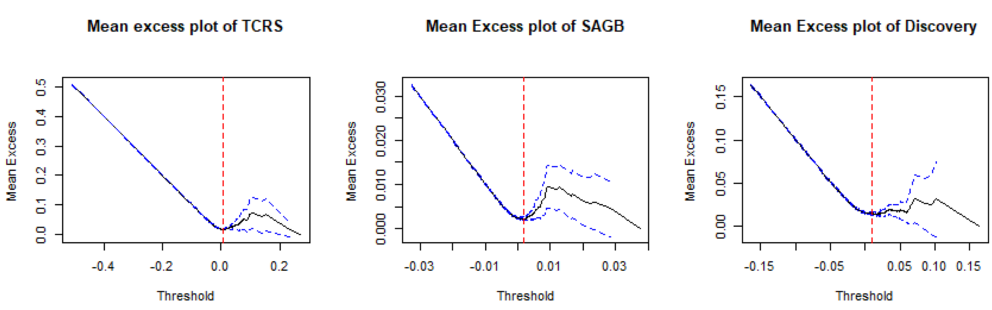


**Fig.4.** Mean excess plots of the datasets.

The mean excess plots of all the three datasets exhibit similar characteristics; consequently, the recommended threshold for the SAGB is within the range of 0 to 0.01, with a slight preference towards the lower end of the spectrum, approximately 0.0035. For Discovery, the suggested threshold is slightly above 0, within the range of 0 to 0.05, particularly around 0.017. Finally, for TCRS, the optimal threshold would be approximately 0.0275. These thresholds have been determined based on the observed turning points in the respective plots, optimising the criteria for the identification of extreme events.

### *3.2.2 Hill plot*

The Hill plot indicates a possible threshold value where the graph first appears to be stable. In Figure 5, these ranges would be indicated by two horizontal lines, meaning that the threshold would be in this range.

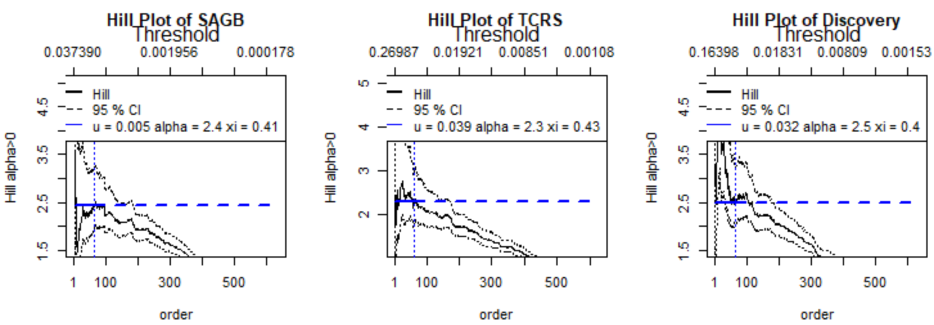


**Fig.5.** Hill plots of the datasets.

The Hill plot conventionally employs order statistics along the $x$-axis, with the $y$-axis representing the Hill estimator values computed for varying orders, that is, each Hill estimator value corresponds to a specific order. In the Hill plots for SAGB, TCRS and Discovery in Figure 5, an apparent commonality emerges in the form of a decreasing trend. This trend is indicative of a finite-tailed distribution, wherein extreme values diminish in extremeness as one progresses further into the tail of the distribution. Moreover, the inclusion of 95% confidence bands encompassing the Hill estimator values within the plots serves the purpose of evaluating the associated uncertainty. Additionally, these confidence bands offer valuable insights into the determination of an appropriate threshold. It is evident from the plots that the threshold value is situated at a relatively low order statistic. The high degree of confidence within this region further strengthens the selection of this threshold. Consequently, the recommended threshold for SAGB, TCRS and Discovery are estimated to be 0.005, 0.039 and 0.032, respectively.

### *3.2.3 Dispersion index plot*

For the dispersion index plot, the goal is to have a dispersion index ratio that is approximately equal to 1, and that is where the threshold value should approximately lie. Thus, for Discovery, TCRS and SAGB, from Figure 6, it appears that the threshold value should be at 0.102, 0.15 and 0.0285, respectively, as it is a point where the dispersion index value is approximately equal to 1.

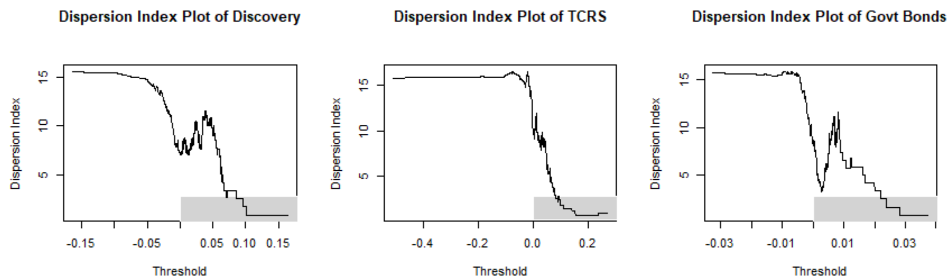


**Fig.6.** Dispersion index plot of all the datasets.

### *3.2.4 Pickand plot*

In the context of Pickand plot, the aim to find a point or an interval where Pickand estimator appears to be smooth. In Figure 7, it is observed that the curve is almost smooth for SAGB, TCRS and Discovery at around 0.0036, 0.027 and 0.024, respectively. Thus, these would be used as the threshold estimates to fit a GPD for $k_n$ greater than these threshold estimates.

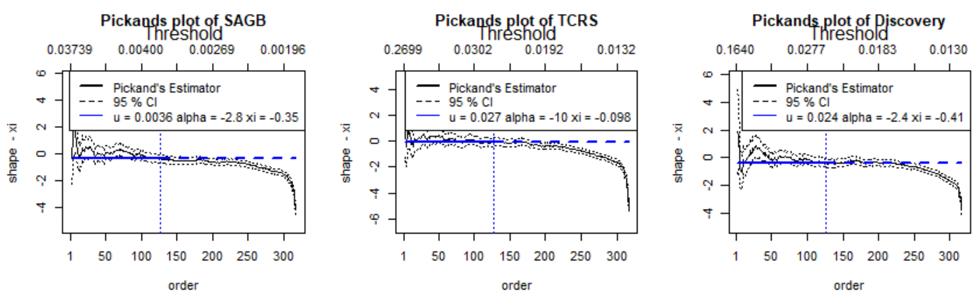


**Fig.7.** Pickand plot for all the datasets.

## 3.3 GPD model fitting

Upon an examination of Table 2, it becomes readily apparent that substantial differences exist among the thresholds estimated through various methods. In this sub-section, we incorporate these different thresholds into our analytical framework so that we can fit the GPD model, as threshold estimate is an essential first step toward this main objective.

**Table 2.** Summary of the thresholds.

| | Mean Excess Function | Hill's plot | Pickand plot | Dispersion index plot |
|---|---|---|---|---|
| **SAGB** | 0.003 | 0.005 | 0.0036 | 0.0285 |
| **Discovery** | 0.017 | 0.032 | 0.024 | 0.103 |
| **TCRS** | 0.0275 | 0.039 | 0.027 | 0.150 |

Subsequently, the fitted GPD parameters were employed to determine the bias inherent in our estimations. The validation of the GPD's appropriateness was accomplished through the utilization of QQ plots. These diagnostic tools enabled a rigorous assessment of the degree to which the GPD model aligned with the empirical data distribution, thus establishing the model's efficiency in capturing the essential characteristics of the extreme events under scrutiny. In this analysis, we use the MSE as our main criterion in deciding the most suitable threshold for a specific dataset, we would also consider the number of threshold exceedances by each threshold value. The goal is to have a relatively smaller MSE and sufficient number of threshold exceedances. It is crucial to note that after we ran this model on empirical datasets, which in this case are datasets $(r_t)$ from Discovery, TCRS and SAGB; we performed multiple simulations from theoretical distributions such as Lognormal, normal and Fréchet distributions to confirm the validity of the conclusions we would draw from the outputs of these empirical datasets.

**Table 3.** GPD empirical properties for all the datasets.

| | | **Mean Excess** | **Pickand plot** | **Hills plot** | **Dispersion Index** |
|---|---|---|---|---|---|
| **SAGB** | Threshold $(u)$ | 0.003 | 0.0036 | 0.005 | 0.0285 |
| | Sample Size | 1265 | 1265 | 1265 | 1265 |
| | No. of Exceedance | 178 | 125 | 63 | 1 |
| | GPD parameter $Shape$ | 0.4062 | 0.39495 | 0.30702 | – |
| | GPD parameter $Scale$ | 0.00149 | 0.00172 | 0.00174 | – |
| | $Variance$ | 49107 | 36512.4 | 36997.35 | – |
| | $Bias^2$ | 6820.56 | 5237.7 | 5271.35 | – |
| | $MSE$ | 55927.6 | 41750.1 | 42268.7 | – |
| **Discovery** | Threshold (u) | 0.0245 | 0.024 | 0.032 | 0.103 |
| | Sample Size | 1265 | 1265 | 1265 | 1265 |
| | No. of Exceedance | 121 | 124 | 65 | 1 |
| | GPD parameter $Shape$ | 0.1474 | 0.1337 | 0.1883 | – |
| | GPD parameter $Scale$ | 0.0134 | 0.01373 | 0.01193 | – |
| | Variance | 138.085 | 131.4 | 85.041 | – |
| | $\text{Bias}^2$ | 13.404 | 16.122 | 10.187 | – |
| | $MSE$ | 151.489 | 147.522 | 95.228 | – |
| **TCRS** | Threshold (u) | 0.0275 | 0.027 | 0.039 | 0.15 |
| | Sample Size | 1265 | 1265 | 1265 | 1265 |
| | No. of Exceedance | 119 | 122 | 59 | 3 |
| | GPD parameter $Shape$ | 0.3185 | 0.3103 | 0.2996 | −1.9645 |
| | GPD parameter $Scale$ | 0.01557 | 0.01568 | 0.17238 | 0.2355 |
| | Variance | 79.31 | 78.65 | 45.123 | 0.64 |
| | $\text{Bias}^2$ | 9.3 | 8.746 | 6.96 | 2984.595 |
| | $MSE$ | 88.61 | 87.396 | 52.083 | 2985.235 |

Firstly, the threshold values from the dispersion index plots (see last column in Table 3) for SAGB and Discovery datasets were disqualified, because these threshold values are too high and they result in only a single exceedance, and therefore it makes no statistical sense to fit a distribution to a single observation. Secondly, the SAGB dataset (which has the lowest volatility), it is observed that the mean excess plot has the highest MSE at 55927.6, while Pickand plot has the lowest MSE at 41750.1. In this case, Pickand plot would be preferred to all other threshold estimation approaches because of its lowest MSE, however we also notice that the MSE value of Pickand plot is not significantly far from the MSE value of Hill's plot, and therefore one might argue that Hill's plot could be used as a proxy to Pickand plot in cases where it is difficult or impossible to carry out Pickand plot approach. Thirdly, for the Discovery dataset (classified as moderately volatile), the mean excess plot yielded a GPD with the highest MSE at 151.489, followed by Pickand plot with the MSE value of 147.522, while the Hill's plot has the lowest MSE value of 95.228, and therefore this would make Hill's plot threshold estimator more preferred than other threshold estimator approaches. Finally, for the TCRS dataset (classified as highly volatile), it is observed that the threshold value from dispersion index plot now yields more than 1 exceedances (observations) which would now enable us to fit a GPD for these threshold values like all other threshold estimates. The MSE for dispersion index plot approach is the highest at 2985.235, and which would make it less preferred in this case. However, the Hill's plot approach has the lowest MSE at 52.083, and therefore it would be more optimal to use.

## 4 Concluding remarks

This study was initiated with the primary goal of estimating thresholds using datasets that encompass different levels of volatility. To be more precise, the principal aim was to determine which threshold estimation method works best with what degree of volatility. Actuarial professionals frequently find themselves in a situation that demands a delicate equilibrium between various stakeholders' requirements. In certain instances, they must determine the best threshold for specific scenarios, such as determining the appropriate level of reinsurance for an insurance company. All these tasks necessitate the skill to harmonize diverse factors. We needed to strike a balance between the variance and bias in attempting to estimate thresholds for extreme values. In our study, we found out that the Pickand plot method for threshold selection produces superior outcomes when the data display relatively low level of volatility. The Hill plot method exhibited an improved performance in situations marked by moderate or high degree of volatility. Overall, with respect to MSE as the main criterion, the Hill plot indicates a significant dominance over all other threshold estimators, even when we are faced with low levels of volatility, still it could be used as a proxy to Pickand plot.

## References

1. A. Chernobai, S. Rachev, F. Fabozzi. *Operational Risk: A Guide to Basel II Capital Requirements, Models, and Analysis.* NJ: John Wiley (2007).
2. J. Beirlant, Y. Goegebeur, J. Segers, J. Teugels. *Statistics of Extremes: Theory and Applications*. Chichester (UK): Wiley (2004).
3. R. Maphalla, M. Mokhoabane, M. Ndou, S.C. Shongwe. In: *Applied Probability Theory-New Perspectives, Recent Advances and Trends*. IntechOpen, London, (2023)
4. D.E. Sanders. *British Int J*, **11**, 519-557 (2005).
5. O. Jakata, D. Chikobvu. *Stat, Optim & Inf Comp*, **8**, 915-933 (2022).
6. S.H. Bhatti, M. Umar, S.C. Shongwe, M. Irfan, M.U. Hassan. *Polish J Envir Stud*. **33** (2024).
7. V.O. Adreev, S.E. Tinykov, O.P. Ovchinnikova, G.P. Parahin. *J Siberian Fed Univ*, 111-121 (2012).
8. P. Sweeting. *Financial Enterprise Risk Management*. Cambridge Univ Press (2011).
9. D. Chikobvu, O. Jakata. *Stat Opt & Info Comp*, **8**, 915-933 (2020).
10. O. Jakata, D. Chikobvu. *J Econ Fin Sci*, **12**, a407 (2019).
11. O. Jakata, D. Chikobvu. *J Stat Appl Prob*, **12**, 1515-1534 (2023).
12. P. Mushori, D. Chikobvu. In: *Cryptocurrencies - Financial Technologies of the Future*. IntechOpen: London (2024).
13. S.I. Hussain, N. Masseran, N. Ruza, M.A. Safari. *J Phys: Conf Ser*, **1988**, 012091 (2021).
14. K.D. Edem, M. Ndengo. *J Fin Risk Manag*, **10**, 225-240 (2021).
15. S. Benito, C. López-Martín, M.Á Navarro. *Risk Manag*, **25** (2023).
16. A. Stephenson. Package 'evd': R package version 2.3-6.1 (2022).
17. C. Scarrott, A. MacDonald. *REVSTAT*, **10**, 33-60 (2012).

18. S. Coles, E. Powel. *Int Stat Rev*, **64** (1996).
19. M.A. Ribatet. A user's guide to the pot package version 1.4 (2006).
20. S. Geman, E. Bienenstock, R. Doursat. *Neural Computation*, **4**, 1-58 (1992).
21. J.D. Cryer, K. Chan. *Time series analysis with applications in R*. Springer (2008).